

Topological analyses and bond characterization of 1,3,5,7-tetra-*tert*-butyl-*s*-indacene: a weak $C_{sp^3}-H \cdots H-C_{sp^2}$ -type dihydrogen interaction

Chih-Chieh Wang,^a Ting-Hua Tang,^b Lai-Chin Wu^b and Yu Wang^{b*}

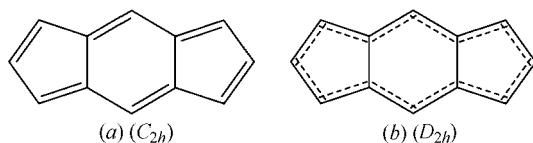
^aDepartment of Chemistry, Soochow University, Taipei, Taiwan, and ^bDepartment of Chemistry, National Taiwan University, Taipei, Taiwan. Correspondence e-mail: yuwang@xtal.ch.ntu.edu.tw

Topological analyses of experimental and theoretical calculated electron densities of 1,3,5,7-tetra-*tert*-butyl-*s*-indacene provide bond characterizations of the chemical bond and of the π -delocalization. A weak $C_{sp^3}-H \cdots H-C_{sp^2}$ -type intramolecular dihydrogen interaction (DHI) is identified through this analysis.

© 2004 International Union of Crystallography
Printed in Great Britain – all rights reserved

1. Introduction

s-Indacene is known as an anti-aromatic 12-membered fused-ring hydrocarbon molecule with 12 π electrons on the ring. It is highly reactive and has not been structurally characterized (Hafner *et al.*, 1963; Hafner, 1982; Hafner *et al.*, 1986; Dunitz *et al.*, 1988). Numerous theoretical calculations have been performed on parent and substituted *s*-indacene to determine whether the suitable geometric structure should be either the localized (*a*) or the delocalized (*b*) form (Nakajima *et al.*, 1964, 1972; Heilbronner & Yang, 1987; Gellini *et al.*, 1993; Kataoka, 1993; Hertwig *et al.*, 1994, 1995; Nendel *et al.*, 1999).



The molecular-orbital calculation at the second-order Moller–Plesset (MP2) level and a complete active space self-consistent field (CASSCF) single-point calculation based on the optimized geometries obtained from the MP2 calculation predicted that a localized structure (*a*) is more stable than the delocalized structure (*b*) by 2.9 and 23.9 kJ mol^{-1} , respectively (Hertwig *et al.*, 1994), but a complete active space second-order perturbation (CASPT2) calculation suggested that the delocalized one (*b*) is more stable by 13.0 kJ mol^{-1} (Hertwig *et al.*, 1994). Some density functional calculations (DFT) also indicated that the delocalized structure (*b*) is more stable (Hertwig *et al.*, 1994, 1995). A quasi-delocalized model for *s*-indacene was proposed (Nendel *et al.*, 1999) after the analyses of geometries, energies and magnetic properties obtained by DFT calculation with non-local corrections of Becke's (1993) three-parameter hybrid method applied to the correlation correction function by Lee, Yang & Parr (LYP) (Lee *et al.*, 1988) (B3LYP). The effects exerted by substituents have been examined for *s*-indacene, the interconversion barrier between the localized and delocalized forms is less than 8 kJ mol^{-1} in the case of 1,3,5,7-tetra-*tert*-alkyl-*s*-inda-

cene (Nendel *et al.*, 1999). 1,3,5,7-Tetra-*tert*-butyl-*s*-indacene (Hafner *et al.*, 1963) is stable in the solid state and was structurally characterized by single-crystal X-ray diffraction both at room temperature (Hafner *et al.*, 1963; Hafner, 1982; Hafner *et al.*, 1986) and at 100 K (Dunitz *et al.*, 1988). Electron-density distributions derived from the experimental charge density and extended Hückel molecular-orbital (EHMO) calculations were studied previously (Wang & Wang, 1991). The molecular-orbital analyses of π bonds in that study yield nine occupied π -bonding orbitals where the extra π orbitals are due to the participation of p - π orbitals of $C\alpha$ atoms bonded to the ring. Such a contribution of substituents on the π delocalization seems to provide a good reason for the stability of the title compound, since 18 π electrons fit in the aromatic criteria. The molecular geometry is essentially in D_{2h} symmetry according to the bond lengths and angles, which are indicative of a delocalized form with aromaticity. It is even predicted so for the singlet and triplet excited states (Gellini *et al.*, 1995) as well as for the dianion case (Cary *et al.*, 1997). Though the relationship between geometry and the localized–delocalized π system of *s*-indacene has been discussed for a long time, the conclusion still remains unclear. In this work, we wish to apply the topological analyses on the molecular electron density obtained from single-crystal X-ray diffraction and from the density functional theory in order to characterize this localized–delocalized mystery. To our surprise, a weak $C-H \cdots H-C$ dihydrogen interaction was detected during the topological analysis. This is, to our knowledge, the first $C_{sp^3}-H \cdots H-C_{sp^2}$ -type intramolecular DHI between the benzenoid H atom and that of the *tert*-butyl group.

2. Experimental and computational details

The molecular structure and the DHI are illustrated in Fig. 1. The experimental electron density was derived from the single-crystal X-ray diffraction data (Dunitz *et al.*, 1988; Wang & Wang, 1991) using the multipole model (Hansen & Coppens, 1978). A single crystal of size $0.14 \times 0.27 \times 0.36$ mm

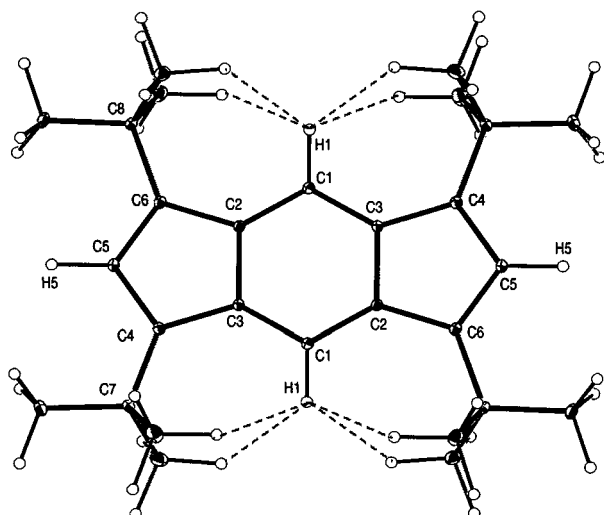
Table 1

Agreement indices of least-squares refinements.

	Model 1†	Model 2‡
NV	368	403
R_1	0.037	0.034
R_{1w}	0.028	0.020
R_2	0.043	0.034
R_{2w}	0.027	0.037
S	1.264	1.294

† The C atoms are up to octapole and H atoms up to dipole, the refinement is based on F^2 (from Wang & Wang, 1991). ‡ Additional H-atom thermal parameters and quadruple terms for hydrogen-bonded atoms. $R_1 = \sum |F_o - kF_c| / \sum F_o$; $R_{1w} = [\sum w|F_o - kF_c|^2 / \sum wF_o^2]^{1/2}$; $R_2 = \sum |F_o^2 - kF_c^2| / \sum F_o^2$; $R_{2w} = [\sum w|F_o^2 - kF_c^2|^2 / \sum wF_o^4]^{1/2}$; $S = [\sum w|F_o^2 - kF_c^2|^2 / \text{NO} - \text{NV}]^{1/2}$; NV: number of variables; NO: number of reflections.

was selected for measurement of diffraction data at 100 K, using a CAD4 diffractometer. The data were collected up to 2θ of 84° ; many symmetry-equivalent reflections and reflections with different ψ values were collected. 22668 measurements were performed in total, which led to 5636 reflections after averaging of the equivalents. The interset agreement index $\sum \Delta I_i / \sum I_i$ is 0.02. Multipole refinements were reinvestigated using the XD program system (Koritsanzsky *et al.*, 1996). The actual molecule symmetry is C_i . The C and H atoms were refined anisotropically and isotropically, respectively. The levels of multipole expansion were made up to octapole and dipole for C and H atoms, respectively, but up to quadrupole for hydrogen-bonded atoms. All the *tert*-butyl H atoms were constrained to be the same. The minimizing function is based on F^2 . During the refinement, the H atom is moved along the C–H vector to make a C–H distance of 1.08 Å (Dunitz & Seiler, 1983; Wang *et al.*, 1987). The agreement indices based on 5394 observed [$F^2 \geq 3\sigma(F^2)$] reflections are listed in Table 1, together with those from the previous refinement (Wang & Wang, 1991). There is only a little improvement in agreement indices for the additional 35 parameters. The residual density map is displayed in Fig. 2; it is essentially featureless. The

**Figure 1**

The molecular structure and intramolecular dihydrogen bond interactions (DHIs) of the title compound.

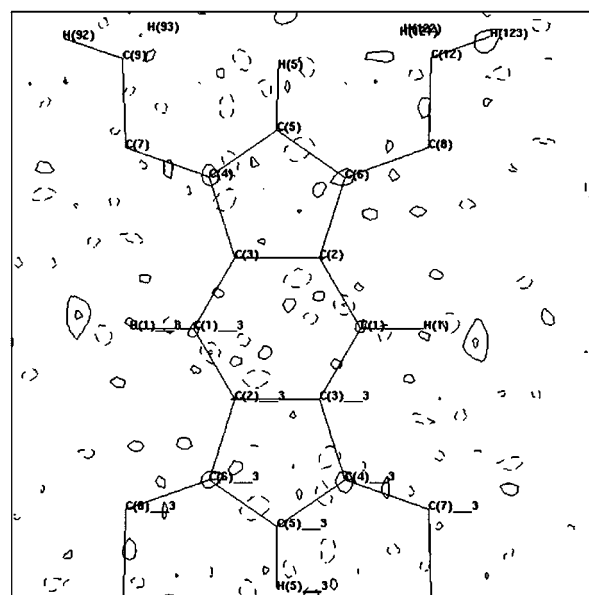
Table 2

Properties associated with bond critical points for selected bonds: first line from experiment; second line from DFT calculation.

Bond	$d1^\dagger$	$\rho(\mathbf{r}_c)$	$\nabla^2\rho(\mathbf{r}_c)$	ε^\ddagger	$H(\mathbf{r}_c)^\S$
bond length (Å)	(Å)	(e Å ⁻³)	(e Å ⁻⁵)		(Hartree Å ⁻³)
C1–C2	0.69	2.13 (2)	–16.47 (4)	0.22	–2.312
1.400 (1)	0.72	2.01	–20.25	0.20	–2.080
C1–C3	0.72	2.16 (3)	–17.10 (6)	0.28	–2.351
1.400 (1)	0.72	2.01	–20.25	0.20	–2.080
C2–C3	0.71	2.05 (1)	–14.73 (4)	0.19	–2.124
1.446(1)	0.72	1.87	–17.54	0.16	–1.790
C3–C4	0.70	1.92 (1)	–12.88 (4)	0.17	–1.960
1.443 (1)	0.71	1.85	–17.12	0.16	–1.772
C4–C5	0.71	2.17 (2)	–16.53 (4)	0.21	–2.346
1.410 (1)	0.71	1.99	–19.44	0.22	–2.039
C2–C6	0.73	1.97 (2)	–13.61 (4)	0.18	–2.033
1.441 (1)	0.72	1.84	–16.93	0.16	–1.755
C5–C6	0.71	2.08 (2)	–14.46 (4)	0.25	–2.206
1.411 (2)	0.90	1.98	–19.18	0.22	–2.013
C6–C8	0.78	1.76 (1)	–9.92 (3)	0.07	–1.635
1.517 (1)	0.78	1.65	–14.43	0.03	–1.408
C8–C14	0.77	1.66 (1)	–8.12 (3)	0.05	–1.479
1.540 (1)	0.77	1.55	–12.74	0.01	–1.261
C1–H1	0.70	1.93 (6)	–17.0 (3)	0.03	–1.991
1.077 (2)	0.68	1.89	–25.78	0.00	–2.093
C5–H5	0.71	1.84 (3)	–16.34 (9)	0.09	–1.885
1.076 (2)	0.67	1.87	–25.15	0.03	–2.067
C14–H141	0.67	1.88 (2)	–17.48 (5)	0.10	–1.943
1.079 (2)	0.67	1.86	–24.39	0.01	–2.048
C14–H143	0.68	1.94 (2)	–19.03 (5)	0.09	–2.048
1.080 (2)	0.67	1.84	–24.04	0.01	–2.022

† $d1$: distances from BCP to the first atom of the bond. ‡ ε is the ellipticity $(|\lambda_1/\lambda_2| - 1)$. § $H(\mathbf{r}_c)$ is the total energy density at the BCP. Estimated with Abramov expression for hydrogen bonds at BCP (Abramov, 1997; Espinosa *et al.*, 1998).

theoretical electron density was derived from a DFT calculation based on the B3LYP functional together with the 6-31G(d,p) basis functions. All the calculations were carried out using the GAUSSIAN98 program (Frisch *et al.*, 1998). In

**Figure 2**

The residual map at the molecular plane. The contour interval is 0.1 e \AA^{-3} ; the solid line shows positive and dashed line negative contours.

order to estimate the stabilization energy due to the DHI, an additional MP2/6-31G(d,p)//B3LYP/6-31G(d,p) calculation based on the optimized geometry was performed in which the methyl groups of the *tert*-butyl substituents were rotated 60° to destroy the DHI. Although the optimized geometry is essentially the same as the experimental one, the biggest difference is less than 0.01 Å in bond length.

3. Results and discussion

3.1. Laplacian of charge density and topological values at BCPs

The Laplacian of the charge density, $\nabla^2\rho$, in the plane of the 12-membered fused ring from experiment (multipole model) and theory is depicted in Fig. 3. The local charge concentrations (CC) of all the ring C atoms are clearly shown as triangular in shape, indicating an sp^2 -type C atom. The shared interaction (or covalent character) of C—C and C—H bonds is also illustrated by the figure. Bond critical points (BCP) (\mathbf{r}_c)

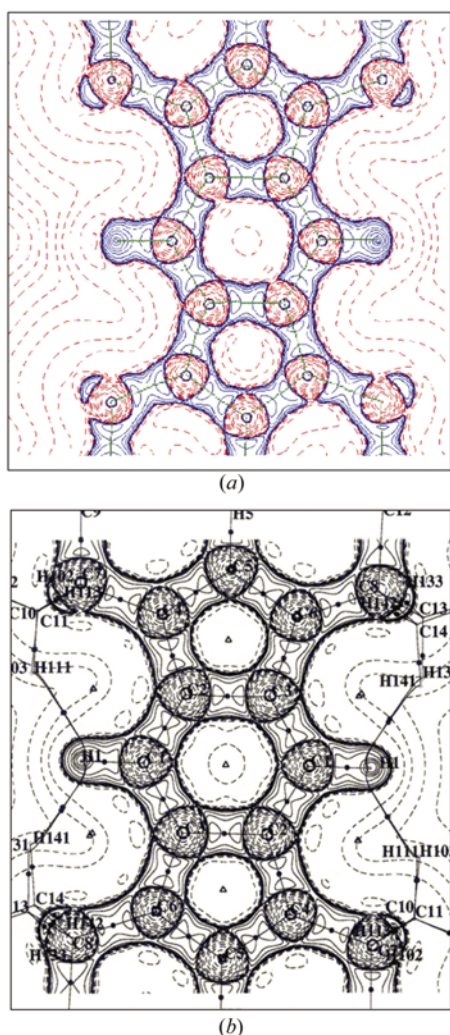


Figure 3 Laplacian maps of the 12-membered fused-ring (a) from experiment, (b) from DFT calculation (solid line negative; dotted line positive). The contours are in steps of $(\pm)2^m 10^n$ ($l = 1, 0; m = 1-3; n = -3$ to $+3$) $e \text{ \AA}^{-5}$.

and the associated properties for selected C—C and C—H bonds are further detailed in Table 2. Selected C—C bonds and C—H bonds all have relatively high values of $\rho(\mathbf{r}_c)$, negative values of $\nabla^2\rho(\mathbf{r}_c)$ and large negative values of total energy density, $H(\mathbf{r}_c)$, at the corresponding BCPs (Table 2). The total energy density $H(\mathbf{r}_c)$ is defined as $H(\mathbf{r}_c) = G(\mathbf{r}_c) + V(\mathbf{r}_c)$, where $G(\mathbf{r})$ is a local kinetic energy and $V(\mathbf{r})$ is the average field experienced by one electron in a many-particle system. The covalent bonding feature (shared interaction) can be characterized by $H(\mathbf{r}_c) < 0$. On the other hand, the closed-shell interactions, van der Waals interaction or ionic bonds are characterized by a positive $H(\mathbf{r}_c)$ (Bader & Essén, 1984; Bader, 1990; Cremer & Kraka, 1984*a,b*). The agreement between experiment and theory is reasonably good on topological properties. Although the experimental $H(\mathbf{r}_c)$ value is calculated according to Abramov's expression, which is derived for the closed-shell interaction, nevertheless it does seem to give reasonable values for shared interaction as indicated in Table 2 and elsewhere (Lee *et al.*, 2001, 2002, 2003), where the agreement between experiment and theory is reasonably good. This covalent character is also demonstrated in the corresponding Laplacian of density shown in Fig. 3. The relative magnitudes of $\rho(\mathbf{r}_c)$ and $H(\mathbf{r}_c)$ are in accord with the expected bond strength. The bond ellipticity, ϵ , is a good index

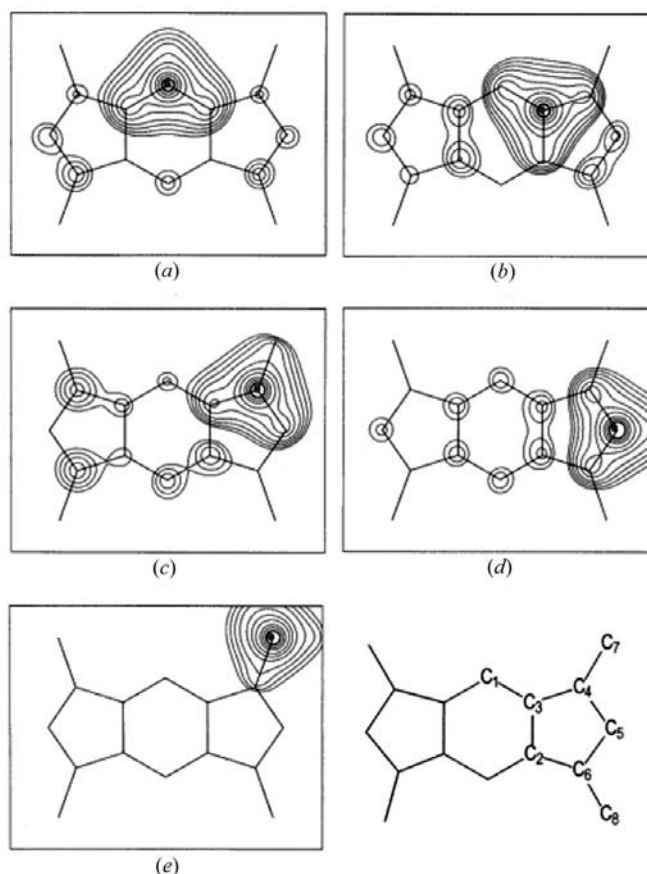


Figure 4 Fermi-hole function calculated by DFT in the plane 0.5 Å above the ring with the reference electron (\bullet) placed in this plane above (a) C1, (b) C3, (c) C4, (d) C5, (e) C7.

Table 3

Topological properties associated with H···H bond critical points: first line from experiment; second line from DFT calculation.

Compound	H···H bond length (Å)	BP (Å)	$d1^\dagger$ (Å)	$\rho(\mathbf{r}_c)$ ($e \text{ \AA}^{-3}$)	$\nabla^2\rho(\mathbf{r}_c)$ ($e \text{ \AA}^{-5}$)	$H(\mathbf{r}_c)$ (kJ mol^{-1})	$G(\mathbf{r}_c)$ (kJ mol^{-1})
1,3,5,7-Tetra- <i>tert</i> -butyl- <i>s</i> -indacene ^(a)	H1···H103	2.27	1.24	0.040 (5)	0.634 (2)	28.72	87.06
	2.19 (2)	2.35	1.14	0.049	0.733	29.99	131.78
	H1···H111	2.21	1.22	0.045 (5)	0.706 (1)	30.88	97.80
	2.17 (2)	2.35	1.14	0.049	0.733	29.99	131.78
	H1···H131	2.28	1.20	0.052 (6)	0.743 (2)	30.04	105.97
	2.19 (2)	2.35	1.14	0.049	0.733	29.99	131.78
	H1···H141	2.24	1.18	0.059 (6)	0.750 (2)	27.07	110.77
2.19 (2)	2.35	1.14	0.049	0.733	29.99	131.78	
9,10-Dihydrophenanthrene ^(b)	2.146	2.42		0.068	1.066	49.84	147.74
Tetra- <i>tert</i> -butylcyclobutadiene ^(b)	1.805	1.83		0.113	1.238	12.46	215.37
	1.857	1.88		0.103	1.156	17.80	195.79
	2.313	2.41		0.046	0.606	26.70	85.44
	2.220	2.30		0.054	0.715	28.50	103.24
<i>cis</i> -HMn(CO) ₄ PPh ₃ ^(c)	2.101(3)	2.12	1.07	0.066	0.790		
[Ir(H ₃)(PH ₃)(NHCH ₂ NH ₂)] ^(d)	1.929 (HF)			0.108	0.990		
	1.818 (MP2)			0.149	1.062		
[(BH ₃ NH ₃) ₂] ^(e)	1.914 (HF)			0.085	0.852		
	1.726 (MP2)			0.128	1.120		
	2.324 (HF)			0.045	0.596		
	2.149 (MP2)			0.065	0.838		

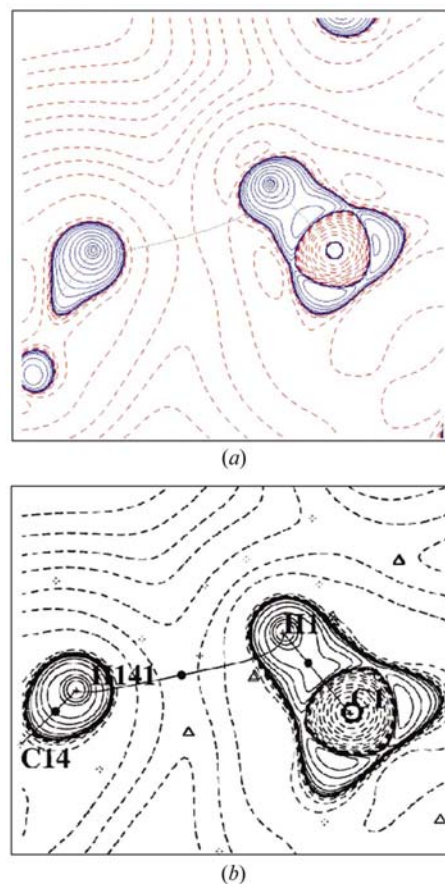
† $d1$: distances from BCP to the first atom of the bond. References: (a) This work; (b) Matta *et al.* (2003); (c) Abramov *et al.* (1998); (d) Calhorda & Lopes (2000); (e) Popelier (1998).

of the π delocalization. The ε values of the C—C bonds in the five- and six-membered rings are in the range of 0.16–0.28 for the experiment and in theory, which is in good agreement with the calculated value in benzene (0.23) (Bader, 1990). It reflects the existence of π delocalization in the *s*-indacene ring.

3.2. Fermi-hole distribution

Such delocalization can be further confirmed by the Fermi-hole distribution. The Fermi-hole function (McWeeny, 1960; Bader & Stephens, 1974, 1975) is a distribution function for an electron of a given spin that determines the decrease in the probability of finding another electron with the same spin relative to a fixed position of the electron in question (reference electron). Thus the Fermi-hole function describes the region where the charge of the reference electron is spread out in space. It was demonstrated (Bader, Johnson *et al.*, 1996) that a physical measure of electron localization or delocalization could be determined by the corresponding localization or delocalization of the Fermi-hole function (Bader, Streitwieser *et al.*, 1996; Hwang & Wang, 1998; Lee *et al.*, 1999, 2001). Fermi-hole functions calculated by DFT are depicted in Fig. 4 with the reference electron (●) located 0.5 Å above the ring plane of *s*-indacene at various C-atom sites. Although the actual symmetry is C_{2v} , it is pseudo D_{2h} according to Fermi-hole distribution, therefore only the typical ones are shown here. It is clearly shown that the π delocalization is distributed over the ring C atoms as illustrated in Fig. 4, where the Fermi-hole distributions are shown over all the ring C atoms when the reference electron is located at either the six-membered ring (Fig. 4*a*, *b*) or the five-membered ring C atoms (Fig. 4*c*, *d*). However, the C atom of the *tert*-butyl group does not participate in this π delocalization as evidenced in Fig. 4(*e*). This does not support the earlier prediction of 18 π -electron delocalization (Wang & Wang, 1991). The description of the

electronic structure of *s*-indacene should therefore be a totally symmetric delocalization involving the 12 C atoms of the ring skeleton as proposed in scheme (*b*).

**Figure 5**

Laplacian maps and bond paths in the C(1)–H(1)···H(141) plane. The definitions of (*a*) and (*b*) and the contours are as in Fig. 3.

3.3. Laplacian and topological properties of C—H···H—C dihydrogen interaction

The atoms in molecules (AIM) approach has provided a way to search for weak interactions, for example, the detection of hydrogen bonds (HBs) (Calhorda, 2000, and reference therein; Flaig *et al.*, 2002). Recently, this approach has been successfully applied to a new type of hydrogen bond, a dihydrogen bond (DHB) dominated by the electrostatic interaction between two H atoms of opposite charge (Peris *et al.*, 1995; Richardson *et al.*, 1995; Custelcean & Jackson, 2001), such as $X-H\cdots H-M$ ($M = \text{Ir}, X = \text{O}, \text{N}; M = \text{Mn}, X = \text{C}$) (Abramov *et al.*, 1998; Calhorda & Lopes, 2000), or $D-H\cdots H-A$ ($D = \text{O}, \text{N}, A = \text{B}; D = \text{F}, A = \text{Li}, \text{Na}, \text{Be}, \text{Mg}, \text{C}, \text{Si}$) (Popelier, 1998; Grabowski, 2000*a,b*). It is important to note the features that distinguish DHI from DHB; in DHI, both H atoms in the $H\cdots H$ interaction exhibit identical or similar polarity. There are eight $H\cdots H$ dihydrogen interactions identified in this molecule through the AIM approach as indicated in Fig. 1. The topological analysis on electron density indicates the existence of BCPs and the corresponding bond paths (BPs) linking each of the apical benzenoid H atoms to four methyl H atoms of *tert*-butyl groups. Such a $C_{sp^2}-H\cdots H-C_{sp^3}$ -type DHI was also pointed out recently in a theoretical approach (Matta *et al.*, 2003). The $H\cdots H$ distances are in the range 2.17 (2)–2.19 (2) Å. Similar homonuclear DHB of $M-H\cdots H-M$ were found with an $H\cdots H$ distance of 2.29 Å in $\text{HMn}(\text{CO})_5$ (LaPlace *et al.*, 1969; McNeill & Scholer, 1977) and 2.12 Å in $[(\eta^5-C_5H_5)_2Zr(\mu-H)(\text{OSO}_2\text{CF}_3)]_2 \cdot 0.5\text{THF}$ (Luistra *et al.*, 1995). The relevant topological properties of $H\cdots H$ bond critical points of some compounds are listed in Table 3. The suspiciously low standard deviations in $\rho(\mathbf{r}_c)$ and $\nabla^2\rho(\mathbf{r}_c)$ may be due to the positional parameters of H atoms being fixed. The existence of such a DHI is also identified through the location of $H\cdots H$ BCP and the associated BP together with the location of the ring critical point, which are shown in Fig. 5. Unlike the C—C and C—H bonds, the bent bond with BP greater than the corresponding bond length (BL) was found for such DHI, as shown in Table 3 and Fig. 5. This DHI is a typical closed-shell interaction. To our knowledge, this is the first case of a homonuclear $C_{sp^3}-H\cdots H-C_{sp^2}$ type of intramolecular DHI. The extra eight $C_{sp^3}-H\cdots H-C_{sp^2}$ intramolecular DHIs do provide the stabilization energy of 130.06 kJ mol⁻¹ for this compound. The binding energy, 16.24 kJ mol⁻¹, for such weak $H\cdots H$ interaction is comparable with those of 13.0 and 19.3 kJ mol⁻¹ for 9,10-dihydrophenanthrene and tetra-*tert*-butyl-cyclobutadiene (Matta *et al.*, 2003), respectively, and is larger than some weak intermolecular bonding interactions, e.g. $C\cdots S'$ and $O\cdots N'$ with 9.42 and 5.78 kJ mol⁻¹, respectively (Lee *et al.*, 2003). Based on this, we may provide a reason why the tetra-*tert*-butyl-*s*-indacene is stable in the solid state, but *s*-indacene is thermally unstable.

In conclusion, the 12 π -electron delocalization of the system is confirmed through the topological analyses of the electron-density distributions both in experiment and in theory. The additional Fermi-hole function from the DFT calculation

further illustrates such π delocalization on the ring C atoms. The stabilization of the title compound in the solid state is rationalized through the existence of eight intramolecular $C_{sp^3}-H\cdots H-C_{sp^2}$ DHIs.

References

- Abramov, Y. A. (1997). *Acta Cryst.* **A53**, 264.
 Abramov, Y. A., Brammer, L., Klooster, W. T. & Bullock, R. M. (1998). *Inorg. Chem.* **37**, 6317.
 Bader, R. F. W. (1990). *Atoms in Molecules. A Quantum Theory*. New York: Oxford University Press.
 Bader, R. F. W. & Essén, H. (1984). *J. Chem. Phys.* **80**, 1943–1960.
 Bader, R. F. W., Johnson, S., Tang, T.-H. & Popelier, P. L. (1996). *J. Chem. Phys.* **100**, 15398–15415.
 Bader, R. F. W. & Stephens, M. E. (1974). *Chem. Phys. Lett.* **26**, 445.
 Bader, R. F. W. & Stephens, M. E. (1975). *J. Am. Chem. Soc.* **97**, 7391.
 Bader, R. F. W., Streitwieser, A., Neuhaus, A., Laidig, K. E. & Speers, P. (1996). *J. Am. Chem. Soc.* **118**, 4959–4965.
 Becke, A. D. (1993). *J. Chem. Phys.* **98**, 5648–5652.
 Calhorda, M. J. (2000). *Chem. Commun.* pp. 801–809.
 Calhorda, M. J. & Lopes, P. E. M. (2000). *J. Organomet. Chem.* **609**, 53.
 Cary, D. R., Green, J. C. & O'Hare, D. (1997). *Angew. Chem. Int. Ed. Engl.* **36**, 2618–2620.
 Cremer, D. & Kraka, E. (1984*a*). *Angew. Chem. Int. Ed. Engl.* **23**, 627.
 Cremer, D. & Kraka, E. (1984*b*). *Croat. Chem. Acta*, **57**, 1259.
 Custelcean, R. & Jackson, J. E. (2001). *Chem. Rev.* **101**, 1963–1980.
 Dunitz, J. D., Krüger, C., Irgartinger, H., Maverick, E. F., Wang, Y. & Nixdorf, M. (1988). *Angew. Chem. Int. Ed. Engl.* **27**, 387–389.
 Dunitz, J. D. & Seiler, P. (1983). *J. Am. Chem. Soc.* **105**, 7056–7058.
 Espinosa, E., Molins, E. & Lecomte, C. (1998). *Chem. Phys. Lett.* **285**, 170.
 Flaig, R., Koritsanszky, T., Dittrich, B., Wagner, A. & Luger, P. (2002). *J. Am. Chem. Soc.* **124**, 3407–3417.
 Frisch, M. J., Trucks, G. W., Schlegel, H. B., Scuseria, G. E., Robb, M. A., Cheeseman, J. R., Zakrzewski, V. G., Montgomery, J. A., Stratmann, R. E., Burant, J. C., Dapprich, S., Millam, J. M., Daniels, A. D., Kudin, K. N., Strain, M. C., Farkas, O., Tomasi, J., Barone, V., Cossi, M., Cammi, R., Mennucci, B., Pomelli, C., Adamo, C., Clifford, S., Ochterski, J., Petersson, G. A., Ayala, P. Y., Cui, Q., Morokuma, K., Malick, D. K., Rabuck, A. D., Raghavachari, K., Foresman, J. B., Cioslowski, J., Ortiz, J. V., Stefanov, B. B., Liu, G., Liashenko, A., Piskorz, P., Komaromi, I., Gomperts, R., Martin, R. L., Fox, D. J., Keith, T., Al-Laham, M. A., Peng, C. Y., Nanayakkara, A., Gonzalez, C., Challacombe, M., Gill, P. M. W., Johnson, B. G., Chen, W., Wong, M. W., Andres, J. L., Head-Gordon, M., Replogle, E. S. & Pople, J. A. (1998). *GAUSSIAN98, Revision A.7*. Gaussian, Inc., Pittsburgh, PA, USA.
 Gellini, C., Angeloni, L. & Salvi, P. R. (1995). *J. Phys. Chem.* **99**, 85–93.
 Gellini, C., Cardini, G., Salvi, P. R., Marconi, G. & Hafner, K. (1993). *J. Phys. Chem.* **97**, 1286–1293.
 Grabowski, S. J. (2000*a*). *Chem. Phys. Lett.*, **327**, 203.
 Grabowski, S. J. (2000*b*). *J. Phys. Chem. A*, **104**, 5551.
 Hafner, K. (1982). *Pure Appl. Chem.* **54**, 939–956.
 Hafner, K., Häfner, K. H., Köning, C., Kreuder, M., Ploss, G., Schultz, G., Sturm, E. & Vöpel, K. H. (1963). *Angew. Chem. Int. Ed. Engl.* **1963**, 2, 123–134.
 Hafner, K., Stowasser, B., Krimmer, H. P., Fischer, S., Böhm, M. C. & Lindner, H. J. (1986). *Angew. Chem. Int. Ed. Engl.* **25**, 630–632.
 Hansen, N. K. & Coppens, P. (1978). *Acta Cryst.* **A34**, 909–921.
 Heilbronner, E. & Yang, Z. Z. (1987). *Angew. Chem. Int. Ed. Engl.* **26**, 360–362.
 Hertwig, R. H., Holthausen, M. C., Koch, W. & Maksić, Z. B. (1994). *Angew. Chem. Int. Ed. Engl.* **33**, 1192–1194.

- Hertwig, R. H., Holthausen, M. C., Koch, W. & Maksić, Z. B. (1995). *Int. J. Quantum Chem.* **54**, 147–159.
- Hwang, T. S. & Wang, Y. (1998). *J. Phys. Chem. A*, **102**, 3276–3731.
- Kataoka, M., (1993). *J. Chem. Res. Synop.* pp. 104–105.
- Koritsanzky, T., Howard, S., Richter, T., Su, Z., Mallinson, P. R. & Hansen, N. K. (1996). *XD Computer Program Package for Multipole Refinement and Analysis of Electron Densities from X-ray Diffraction Data*. Free University of Berlin, Germany.
- La Place, S. J., Hamilton, W. C., Ibers, J. A. & Davison, A. (1969). *Inorg. Chem.* **8**, 1928.
- Lee, C., Yang, W. & Parr, R. G. (1988). *Phys. Rev. B*, **37**, 785–789.
- Lee, C. R., Tan, L. Y. & Wang, Y. (2001). *J. Phys. Chem. Solids*, **62**, 1613–1628.
- Lee, C. R., Tang, T.-H., Chen, L. & Wang, Y. (2003). *Chem. Eur. J.* **9**, 3112–3121.
- Lee, C. R., Wang, C. C., Chen, K. C., Lee, G. H. & Wang, Y. (1999). *J. Phys. Chem. A*, **103**, 156–165.
- Lee, J. J., Lee, G. H. & Wang, Y. (2002). *Chem. Eur. J.* **8**, 1821–1832.
- Luistra, G. A., Rief, U. & Prosenc, M. H. (1995). *Organometallics*, **14**, 1551.
- McNeill, E. & Scholer, F. R. (1977). *J. Am. Chem. Soc.* **99**, 6243.
- McWeeny, R. (1960). *Rev. Mod. Phys.* **32**, 335.
- Matta, C., Hernández-Trujillo, J., Tang, T.-H. & Bader, R. F. W. (2003). *Chem. Eur. J.* **9**, 1940.
- Nakajima, T., Saijo, T. & Yamaguchi, H. (1964). *Tetrahedron*, pp. 2119–2124.
- Nakajima, T., Toyota, A. & Fujii, S. (1972). *Bull. Chem. Soc. Jpn*, **45**, 1022–1029.
- Nendel, M., Goldfuss, B., Houk, K. N. & Hafner, K. (1999). *J. Mol. Struct. (Theochem)*, **461–462**, 23–28.
- Peris, E., Lee, J. C., Rambo, J. E., Eisenstein, O. & Crabtree, R. H. (1995). *J. Am. Chem. Soc.* **117**, 3485–3491.
- Popelier, P. L. A. (1998). *J. Phys. Chem. A*, **102**, 1873.
- Richarson, T. B., de Gala, S., Crabtree, R. H. & Siegbahn, P. E. M. (1995). *J. Am. Chem. Soc.* **117**, 12875–12876.
- Wang, Y., Angermund, K., Goddard, R. & Kruger, C. (1987). *J. Am. Chem. Soc.* **109**, 587–589.
- Wang, Y. & Wang, C. C. (1991). *J. Chin. Chem. Soc.* **38**, 5–14.